Sakarya University Journal of Science 25(6), 1287-1294, 2021

In-Plane Buckling of Open-section Shell Segments

Haluk YILMAZ*[1], İbrahim KOCABAŞ[1]

Abstract

The present study investigates elastic buckling behavior of open-section shell segments under action of a central radial load. A design parameter is expressed to characterize the influence of fillet radius on load-bearing capacity. A reduction factor equation is developed as a multivariate function of shell parameters, which evaluates the amount of decrease in load-bearing capacity of the structure caused by the corner fillet. In addition, an expression to predict limit load of the shell structure under clamped end conditions is introduced. Furthermore, a parametric study is performed to reveal the influence of fillet radius and radius-to-thickness ratio on the limit load as well as deformation patterns of the open-section shells. Results show that corner fillets have a significant effect on the limit load of the open-section shell segments under in-plane loading.

Keywords: buckling, open-section shell, radial load, load-bearing capacity

1. INTRODUCTION

Buckling of open-section shell segments is a classical stability problem and exact solutions are only available for limited cases, based on certain assumptions. Major practical application of this kind of structures are rigid-concreate pavement substructure for highways, open foundations for buildings, laterally and vertically loaded piles, tunnels in soil profile etc. Since the open-section shell is a special type of an arch profile with an opening angle of 90 degrees, the arch structures in the design of bridges, roofs and applications concerning structural engineering and architecture may be shown as the other examples. A shell-segment with an open section, which is under a central radial load, is also a buckling problem and the shell structure may suddenly lose its stability in a non-linear fashion. For this reason, exact solutions are generally incapable of capturing deformation patterns and load-bearing capacities of these structures. To resolve this issue, the use of numerical analysis is an effective tool because it considers the role of non-linear geometry on the buckling behavior. In addition, geometric parameters of the shell segments play an important role in the load-bearing capacity and equilibrium paths as well as material properties, boundary conditions and loading types. This is because the geometric stiffness is highly dependent to the geometry of the shell structures and the system may lose its stability before reaching the yield point of the material. To analyze the stability of the open-shell segments under radial loading cases, researchers are proposed several analytical approaches. For example, a new theory for the buckling and nonlinear analysis of the thin-walled structures is developed by Chengyi et al., [1] to reflect the

* Corresponding author: halukyilmaz@eskisehir.edu.tr
[1] Eskisehir Technical University, Vocational School of Transportation
E-mail: ibrahimkocabas@eskisehir.edu.tr
ORCID: https://orcid.org/0000-0002-6750-3708, https://orcid.org/0000-0003-0600-2034

influence of shear deformation on the critical load. However, various assumptions based on the Galerkin method are made to obtain analytical solutions of the critical loads. Open or close section shells are the most employed components in many structures. Rao et al. [2] investigate influence of cap fillet of tubular sections on deformation and energy-absorbing characteristics under lateral loading. Their findings emerge that the end fillet details have a strong effect on the deformation patterns and final shape profiles of the tested specimens [2]. This clearly indicates that the buckling response of a shell segment is highly affected by the presence of fillets and their dimensions. A similar study is conducted by Wang et al. [3], to examine vertical shear buckling capacity of steel beams with fillet corner hexagonal web openings. They compared buckling modes and buckling capacities of the beams with hexagonal and circular openings. As a result of their parametric analysis, buckling behavior of the beam is affected by the opening shape, the opening dimension, the opening distance, and thickness [3]. Shell profiles are also an important geometric factor for buckling load evaluations as well as fillet details of corners. Tang et al. [4] are investigated parabolic profiles for buckling load evaluation considering vertical loading cases. A modified eigen-buckling algorithm based on eigenvalue analysis is presented to assess buckling strength of a steel bridge structure regarding to inelastic buckling method and elastic buckling method. They result that influences of the geometric parameters of parabolic arches are taken into account by modifying slenderness parameter [4]. There are several methods to improve buckling loads of thin-walled structures through implementing different geometrical cross-sections. Yang et al. [5] are tried to enhance the local buckling strength of open-section beam segments using some stiffeners in different geometrical forms. They successfully increase the buckling strength up to 207%. This shows importance of geometrical configurations to obtain higher load-bearing capacities in thin-walled structures. On the other hand, type of loading also plays an important role in determining the buckling load of an open-section shell. Pi et al. [6] perform an analytical investigation to reveal significance of pre-buckling behavior of open-section thin-walled arches under uniform radial load. Their numerical results show that the pre-buckling deformations of shallow arches are substantial and neglecting the effects of the pre-buckling deformations will lead to incorrect predictions of the buckling load of the arches. Szychowski [7] apply a warping torsion in an open-section thin-walled structure to investigate the geometry of the cross-section on the buckling characteristics. Pi and Bradford [8] examine stability of circular arches under a sudden uniform radial load. Similar loading case is considered by ref. [9] which takes a radial central load into account to formulate elasto-plastic buckling of arch structures, numerically. A different loading type, which is axial and end moment, is studied by Asadi et al. [10] to investigate buckling behavior of both open and closed section beams. As a result, it is reported that changes in geometrical details and loading types should be precisely considered to develop efficient buckling relations.

This paper aims prediction of in-plane buckling load of an open-section shell segment with different corner fillet radius values subjected to a central radial load, accounting for non-linear geometry. In this case, it would be possible to estimate limit load and reduction factor as a reference to the semi-cylinder profile for a simple open-section shell structure application. For this purpose, buckling load equations under clamped end conditions are developed to predict load-carrying capacities of open-section shell segments. A reduction factor is also proposed to evaluate influence of the corner fillet radius, ranging from a reference circular profile to a rectangular profile, on the load-carrying capacity. In this respect, the present study will have a contribution to the current literature in the field of open-section shell structures.

2. NUMERICAL BUCKLING ANALYSIS

2.1. Open-section Shell Geometry

Geometry of an open-section shell structure is schematically illustrated in Fig. 1. There are four independent geometric parameters in construction of an open-section shell segment which are denoted as shell width L, shell thickness t, fillet radius r and shell height h. A reference circular open-shell profile of radius R as shown in Fig. 1 may be proposed to evaluate the influence of the fillet radius r on the limit load. In this case, for the open-section shell segment, the half-width $L/2$ and the height h are equal to the radius of the reference circular profile ($L=2h=2R$). It enables the buckling load comparisons of the shells with different fillet radius values as a basis of reference shell profile. For general buckling expressions, it is useful to consider normalized geometry parameters. Therefore, normalized parameters, such as ratio of the fillet radius to the radius of reference profile r/R, and radius-to-thickness ratioR/t are chosen for buckling evaluation. The r/R parameter is a geometric shape factor which varies between zero and unity. Several shell configurations are presented in Fig. 2 for different values of r/R. If r/R equals to 1, reference open-section shell profile is constructed. In the case of r/R=0, a rectangular shell section is yielded. A parametric study is conducted to derive buckling expressions for the geometrical open-section shell segment parameters, as can be seen in Table 1.

The geometrical parameters have an extensive range to develop efficient buckling expressions. For this reason, R/t is chosen in the range of 25 and 1000. This is a quite feasible interval considering practical applications of the open-section shells. Similarly, r/R is reasonably taken as between zero and unity with an increment size of 0.1.

Table 1 Range of open-section shell segments for parametric study.

Radius-to-thickness ratio (R/t)	Fillet radius-to-radius of reference profile (r/R)	Young's Modulus E [GPa]
25	0	200
↓	↓	
1000	1	

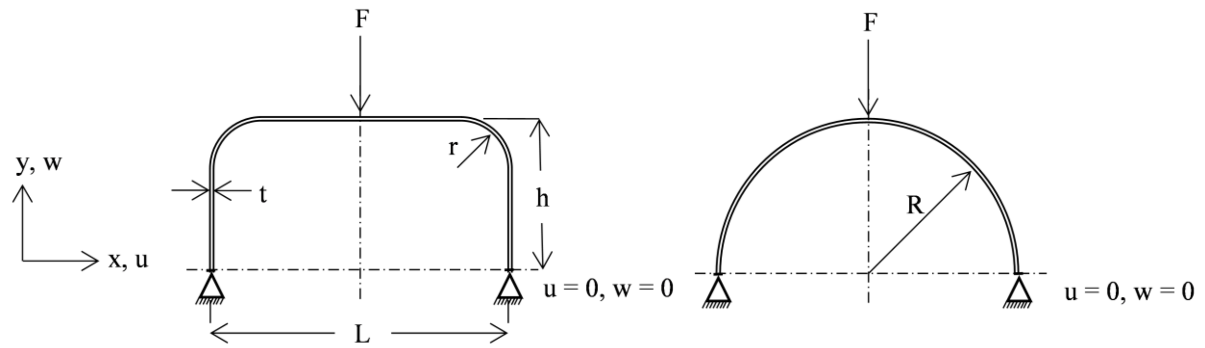

Figure 1 Schematic illustration of an open-section shell geometry with a fillet radius (on left) and reference circular profile (on right).

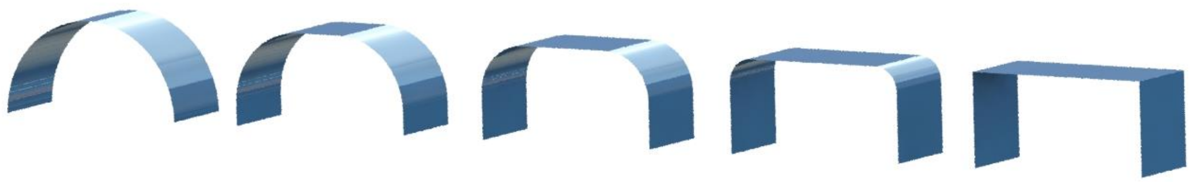

Figure 2 Various open-section shell segment configurations between r/R=1 and r/R=0

2.2. Numerical Model Details

This section gives the details of the finite element model, boundary conditions and numerical analysis. A numerical model is constructed in ANSYS Workbench package program considering static analysis. Fig. 1 displays the boundary conditions employed in the numerical model for fixed (clamped) case. Ends of the shell models are constrained to move in *u* and *w* direction, and a central radial load *F* is applied progressively until the buckling occurrence to simulate in-plane buckling conditions, as shown in Fig 1. The open-section shell system can be modelled as a plane strain problem because the length of the shell is enough large thus out-of-plane buckling is ignored. In this case, the limit load can be expressed as the load per unit depth of the shell in the *z*-direction. A mesh sensitivity analysis is conducted to decide optimal element size considering the accuracy of the numerical analysis. As a result, an element size of 0.25 mm gives reasonably sufficient accuracy because the deviation in the buckling loads does not change considerably for smaller values of the element size. The numerical analysis takes nonlinear geometry referred to GNA (geometrically nonlinear analysis) into account in this study. An elastic material model is considered since the elastic buckling behavior of the shells is investigated. Shell181, four-node quadrilateral shell element with large deflection capability, is selected for the numerical analysis.

The numerical model is validated with the experimental test results in the literature. For this purpose, the experimental test results of limit loads of two semi-cylinder configurations are considered in the validation process [11]. The semi-cylinder dimensions are R=62.5 mm, t=3.2 mm and R=62.5 mm, t=2.4 mm for the first and second test samples, respectively with a depth of 125mm in the *z*-axis. Multilinear material model is implemented in the validation and mechanical properties of the samples are given in ref. [11]. The comparison of numerical and experimental test results is given in Table 2. It is seen that the amount of deviation from the test data is found out to be 10.9% and 5.11% for the first and second semi-cylinder configurations, respectively. Therefore, the proximity between the test data and numerical model is in the acceptable limits.

Table 2 The proximity between experimental and numerical limit load results.

C1	Experimental Limit Load [N/mm]	8.137
	Numerical Limit Load [N/mm]	9.027
	Deviation [%]	10.9
C2	Experimental Limit Load [N/mm]	4.045
	Numerical Limit Load [N/mm]	4.252
	Deviation [%]	5.11

3. RESULTS AND DISCUSSION

The results of numerical analysis of the open-section shell configurations are presented to examine effects of corner fillets on the limit load. Equilibrium paths (load-deflection curves) is an important tool to understand general buckling behavior of a shell structure. For this reason, the load-deflection curves of the shells are plotted in Fig. 3 for the r/R values changing between zero and unity. In the parametric study, R/t varies in the range of 25 and 1000. To demonstrate general buckling behavior, R/t=100 is considered in the construction of the load-deflection diagram in Fig. 3. As can be seen in Fig. 3, a smooth vertical deflection response occurs in which no sharp drops in load-bearing capacity are observed for r/R=0 (rectangular open-section shell segment). As r/R increases up to 0.5, a similar deformation pattern trend is recorded, and relatively higher fluctuations in the load-deflection curve are observed, as shown in Fig. 3. It can be said that the shell structure does not exhibit a significant buckling behavior for the r/R values up to 0.5, which means that the structure almost keeps its load-bearing capacity during loading history. However, a visible reduction is yielded in load-bearing capacity for the r/R values larger than 0.5. Major reason is that the geometric stiffness of the structure does not change considerably up to the limit point in comparison with the configurations where r/R is lower than 0.5, and a membrane stress dominant system is achieved for r/R is greater than 0.5. However, a bending stress dominant system exhibits in the other configurations (r/R<0.5) from beginning of the loading, naturally. In this interval where r/R is between 0.5 and 1, the open-section shell loses its stability, and a limit load value can be directly determined from the diagram. Otherwise, at lower values of *r/R*, the limit load can be determined considering the minimum slope of the equilibrium path. It is notable that the fillet radius *r* has a great impact on the limit load of open-section shells and should be considered as a design factor in the constructions.

Deformation patterns of some selected open-section shell configurations are given in Figs. 4a, 4b and 4c for *r/R*=0, r/R=0.5 and *r/R*=1, respectively. The labels in Fig. 4 represents the total deformation at the buckling instant of the structure. It is seen that the amount of vertical deflection depends on the *r/R* parameter.

However, it is difficult to reach a direct correlation between the limit load and corresponding deflection because *r/R* emerges a nonlinear contribution in terms of buckling behavior. As a result, the mode shapes of the shell configurations are quite similar.

A reference limit load equation is required to measure the amount of reduction in the limit load of the shell structure with a fillet. For this reason, *r/R*=1, which corresponds to a circular shell section, is taken as a reference profile. The limit load of the reference profile, denoted as F_{ref}, is plotted against *R/t*, as shown in Fig. 5. F_{ref} is observed to decrease tremendously as *R/t* increases from 25 to 1000. F_{ref} is apparently a multivariate function of *R/t*, *R* and Young's modulus *E*. Therefore, as a result of the regression process, which is applied to the parametric analysis results, Eq. 1 may be introduced to calculate the limit load of the reference profile per unit depth:

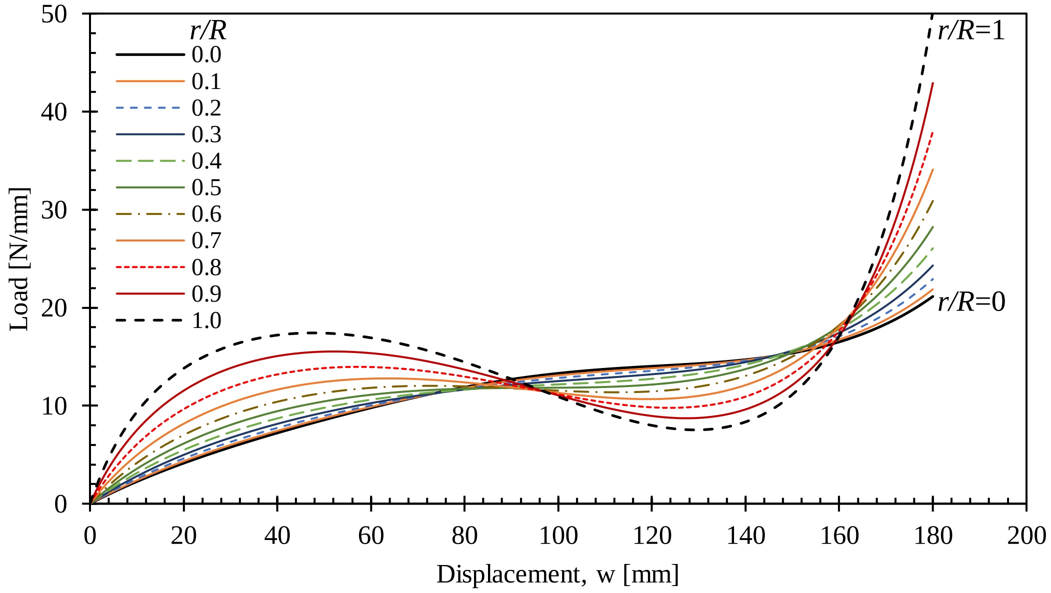

Figure 3 Equilibrium paths (load-deflection diagram) of the open-section shell segment configurations at *R/t*=100.

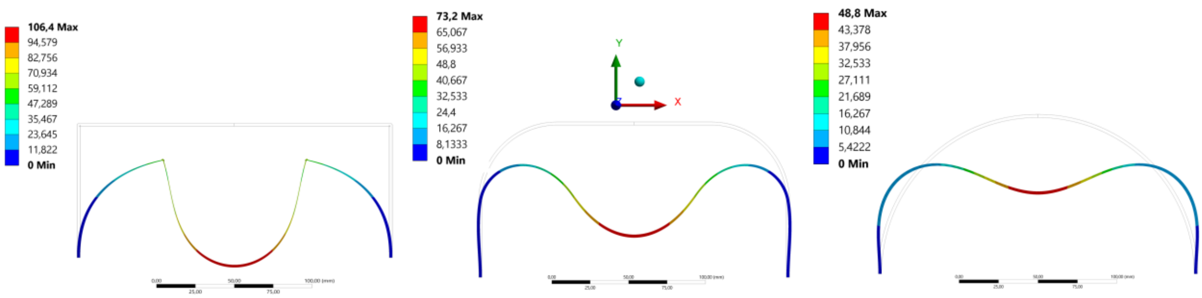

Figure 4 Deformation patterns of the open-section shells for (a) *r/R*=0, (b) *r/R*=0.5 and (c) *r/R*=1.

$$F_{ref} = ER(R/t)^{-3.03} \quad (1)$$

where E is Young's modulus, R is the radius of the reference shell profile and t is the shell thickness.

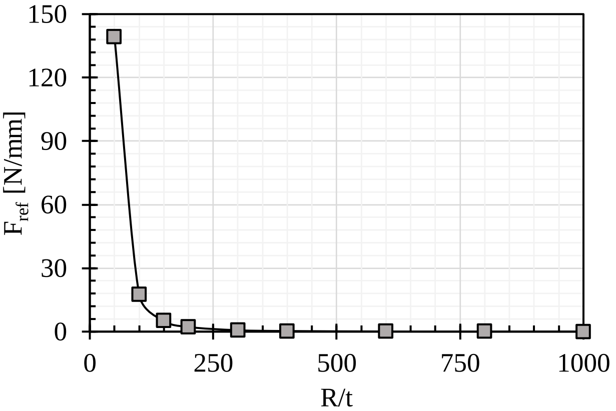

Figure 5 Limit load (F_{ref}) versus *R/t* for the reference open-section shell profile

A reduction factor parameter, which is denoted as φ, is introduced to measure the amount of reduction in the limit load as a basis of reference profile. The reduction factor can be described as $\varphi=F_{lim}/F_{ref}$, where F_{lim} is the limit load of the shell segment for which r/R is lower than unity. To produce an expression, the variation of φ is plotted against *r/R* in the range of 0 to 1, as shown in Fig. 6. The reduction factor φ is calculated based on the limit load values obtained from the numerical analysis. The results emphasize that φ decreases slightly for the increasing values of *r/R* from zero (corresponding to rectangular open-section shell) to 0.5. For 0.5< *r/R* <1, a visible buckling response appears and φ continuously increases as the shell section approaches to reference profile (*r/R* =1). It can be reported that there is a critical region, at around *r/R* =0.5, at which φ reaches some local minima. It means that the maximum decrement appears in the limit load, which is caused by the corner fillets. Although *R/t* is an important parameter in buckling evaluations, it results that there is no considerable influence of *R/t* on the reduction factor. For this reason, an expression for φ may be produced as only a function of *r/R* in the following polynomial form:

$$\varphi = F_{lim}/F_{ref} = 0.9(r/R)^2 - 0.7(r/R) + 0.8 \quad (2)$$

Eq. 2 is proposed as an efficient tool to evaluate the amount of reduction in the limit load of an open-section shell segment which caused by the radius of the corner fillets. Substituting Eq. 1 into Eq.2 and solving for F_{lim} gives the following expression to calculate the limit load of an arbitrary shell configuration:

$$F_{lim} = ER(R/t)^{-3.03}[0.9(r/R)^2 - 0.7(r/R) + 0.8] \quad (3)$$

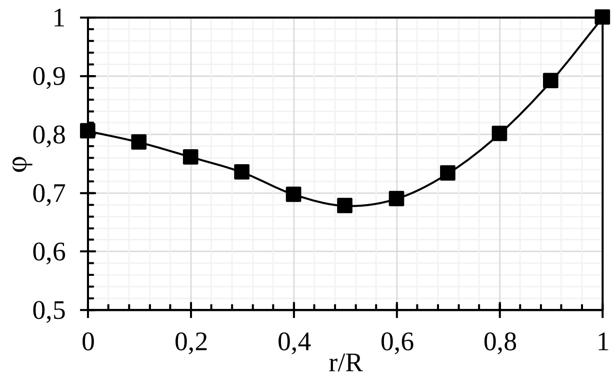

Figure 6 Reduction factor versus *r/R* diagram at *R/t*=100.

A residual estimator approach is implemented as a measure of the accuracy of Eq. 3 as a reference to numerical data. The residual denoted as $\Delta\Phi$ is used as an error indicator. It is expressed as $\Delta\Phi=(F_{num}-F_{eq})/F_{num}$ where F_{eq} and F_{num} are the limit loads obtained from the Eq. 3 and numerical analysis, respectively. $\Delta\Phi$ is presented in Fig. 7 for the *r/R* values in the range of 0 and 1 considering all of the *R/t* values given in Table 1. The horizontal line where $\Delta\Phi$ is equal to zero represents that the predictions obtained from Eq. 3 and numerical analysis are identical. It is concluded that the residuals mostly lay between a lower and upper bound of -0.1 and 0.05, respectively. The higher residuals for each *r/R* ratio are especially obtained at higher *R/t* values. Therefore, the proposed equations give more accurate predictions at lower *R/t* values. However, good proximity is achieved at higher *R/t* with a maximum deviation of +5% and -10%, which is accepted to be in the feasible regions.

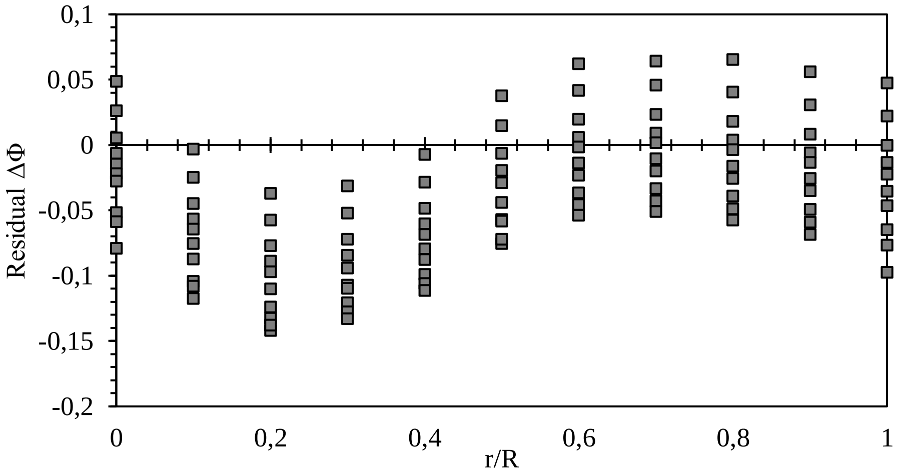

Figure 7 Residual Δϕ versus *r/R* at different *R/t* values in the range of 25 and 1000

4. CONCLUDING REMARKS

In this study, influence of corner fillet radius on the buckling behavior of open-section shell segments under a central radial load is investigated, numerically. The effects of the geometrical parameters on the load-bearing capacity of the open-section shells are studied. Additionally, a parametric study is performed for a wide range of geometry configurations considering clamped boundary conditions. A reduction factor and a limit load equation are developed and compared with the numerical results to examine the accuracy of the equations. Finally, the results that can be drawn from the present study are as follows:

- The load-bearing capacity of an open section shell segment under a radial load varies, which is proportional to (*R/t*)-3.03 for a certain r/R ratio.
- No sudden drop in the load-bearing capacity of the open-section shells is observed for which r/R is lower than 0.5. However, slopes of the equilibrium paths approach to zero just before reaching the stiffening region depending on the change of geometric stiffness
- Limit load attains a maximum value at the semi-circular configuration (reference config.) and a snap-through occurs beyond the limit point as the nature of this kind of structures. It results in a sudden reduction in the load-bearing capacity after the limit point. This is because the geometric stiffness of the semi-circular profile is greater than the other configurations during the loading history.
- Geometric stiffness decreases as the structure turns into to rectangular profile then the severity of the loss of stability diminishes or completely disappears. Nevertheless, the load-bearing capacity of the structure still decreases.
- The limit load may reduce up to 25% depending on *r/R* in connection with the reference profile. It is formulated by a second-order polynomial which evaluates the elastic limit load of the structure without needing a numerical analysis. Therefore, it provides a guide for the selection of an open-section shell geometry with corner fillets according to production and service conditions.

Acknowledgments

The authors are greatly thankful to Eskisehir Technical University, Turkey for providing the facilities in developing the paper.

The Declaration of Conflict of Interest

No conflict of interest or common interest has been declared by the authors.

REFERENCES

[1] C. Chengyi, T. Genshu, and Z. Lei, "In-plane nonlinear buckling analysis of circular arches considering shear deformation," J. Constr. Steel Res., vol. 164, p. 105762, 2020.

[2] M. Gowthamuneswara Rao, A. Praveen Kumar, C. Nagaraj, and L. Ponraj Sankar, "Investigations on the lateral impact behaviour of combined geometry tubular structures and its effect of cap fillet radius," Mater. Today Proc., vol. 27, pp. 1912–1916, 2020.

[3] P. Wang, X. Wang, and N. Ma, "Vertical shear buckling capacity of web-posts in castellated steel beams with fillet corner hexagonal web openings," Eng. Struct., vol. 75, pp. 315–326, 2014.

[4] Z. Tang, W. Zhang, J. Yu, and S. Pospíšil, "Prediction of the elastoplastic in-plane buckling of parabolic steel arch bridges," J. Constr. Steel Res., vol. 168, 2020.

[5] J. Q. Yang, T. Q. Liu, and P. Feng, "Enhancing flange local buckling strength of pultruded GFRP open-section beams," Compos. Struct., vol. 244, p. 112313, 2020.

[6] Y. L. Pi and M. A. Bradford, "Nonlinear dynamic buckling of shallow circular arches under a sudden uniform radial load," J. Sound Vib., vol. 331, no. 18, pp. 4199–4217, 2012.

[7] A. Szychowski, "A theoretical analysis of the local buckling in thin-walled bars with open cross-section subjected to warping torsion," Thin-Walled Struct., vol. 76, pp. 42–55, 2014.

[8] Y. L. Pi and M. A. Bradford, "Elasto-plastic buckling and postbuckling of arches subjected to a central load," Comput. Struct., vol. 81, no. 18–19, pp. 1811–1825, 2003.

[9] Y. L. Pi, M. A. Bradford, and F. Tin-Loi, "Flexural-torsional buckling of shallow arches with open thin-walled section under uniform radial loads," Thin-Walled Struct., vol. 45, no. 3, pp. 352–362, 2007.

[10] A. Asadi, A. H. Sheikh, and O. T. Thomsen, "Buckling behaviour of thin-walled laminated composite beams having open and closed sections subjected to axial and end moment loading," Thin-Walled Struct., vol. 141, pp. 85–96, 2019.

[11] İ. Kocabaş and H. Yılmaz, "In-plane buckling of semi-cylindrical shells with elastic edge restraints under a central radial load," Thin-Walled Struct., vol. 167, pp. 148141, 2021.